RESEARCH ARTICLE

European Journal of **Soil Science** **WILEY**

A root mucilage analogue from chia seeds reduces soil gas diffusivity

Adrian Haupenthal[1,2] | Patrick Duddek[3] | Pascal Benard[3] |
Mathilde Knott[4] | Andrea Carminati[3] | Hermann F. Jungkunst[4] |
Eva Kroener[1,2] | Nicolas Brüggemann[1,2]

[1]Institute of Bio- and Geosciences, Agrosphere (IBG-3), Forschungszentrum Jülich GmbH, Jülich, Germany

[2]Faculty of Agriculture, PhenoRob Cluster of Excellence, University of Bonn, Bonn, Germany

[3]Physics of Soils and Terrestrial Ecosystems, Institute of Terrestrial Ecosystems, ETH Zurich, Zurich, Switzerland

[4]iES Landau, RPTU Kaiserslautern-Landau, Landau, Germany

Correspondence
Adrian Haupenthal, Institute of Bio- and Geosciences, Agrosphere (IBG-3), Forschungszentrum Jülich GmbH, Wilhelm-Johnen-Straße, Jülich, Germany.
Email: a.haupenthal@fz-juelich.de

Funding information
Deutsche Forschungsgemeinschaft, Grant/Award Number: 390732324

Abstract

Gas exchange in the soil is determined by the size and connectivity of air-filled pores. Root mucilage reduces air-filled pore connectivity and thus gas diffusivity. It is unclear to what extent mucilage affects soil pore connectivity and tortuosity. The aim of this study was to gain a better understanding of gas diffusion processes in the rhizosphere by explaining the geometric alterations of the soil pore space induced by mucilage. We quantified the effect of a root mucilage analogue collected from chia seeds without intrinsic respiratory activity on oxygen diffusion at different water contents during drying–rewetting cycles in a diffusion chamber experiment. Quantification of oxygen diffusion showed that mucilage decreased the gas diffusion coefficient in dry soil without affecting air-filled porosity. Without mucilage, a hysteresis in gas diffusion coefficient during a drying–rewetting cycle was observed. The effect depended on particle size and diminished with increasing mucilage content. X-ray computed tomography imaging indicated a hysteresis in the connectivity of the gas phase during a drying–rewetting cycle for samples without mucilage. This effect was attenuated with increasing mucilage content. Furthermore, electron microscopy showed that mucilage structures formed in drying soil increase with mucilage content, thereby progressively reducing the connectivity of the gas phase. In conclusion, the effect of mucilage on soil gas diffusion highly depends on soil texture and mucilage content. The diminishing hysteresis with the addition of mucilage suggests that plant roots secrete mucilage to balance oxygen availability and water content, even under fluctuating moisture conditions.

KEYWORDS

gas diffusion coefficient, hysteresis, liquid bridges, pore connectivity, rhizosphere, root exudates, root respiration, root–soil interactions, X-ray CT

1 | INTRODUCTION

Gas exchange between roots and soil is essential as the O_2 supply from the aerial parts of plants is often insufficient for satisfactory root growth (Gardner et al., 1999) and the accumulation of toxic substances like ethanol and lactic acid near roots can be harmful (Rivoal & Hanson, 1994). Therefore, maintaining gas exchange within the root-rhizosphere-bulk soil system is advantageous for biota in soils.

The movement of gas through soil occurs mainly by diffusion (Gliński & Stępniewski, 1985). Gradients in concentration force gas to move from areas with high concentration to areas with low concentration. This process is controlled by the distribution and connectivity of air-filled pores, and this soil-specific property is represented by the effective diffusion coefficient D_p (Fujikawa & Miyazaki, 2005; Hamamoto et al., 2009). Several studies quantified the effect of soil compaction, water saturation, organic matter and mucilage on gas diffusion and discussed their potential implications (Hamamoto et al., 2012; Haupenthal et al., 2021; Moldrup et al., 2000; Thorbjørn et al., 2008; Xu et al., 1992). Wesseling et al. (1957) stated that a volumetric soil air content of 10% seems to be a threshold for gas diffusion.

Aside from the quantity of water in the soil, its distribution in the pore space affects the connectivity of air-filled pores. Non-uniformity of the pores, entrapped air and a difference in contact angle between the pore water and the interface of soil particles during drying and rewetting, affect the distribution of water, resulting in an effect known as hysteresis (Cooper et al., 2017; Haines, 1930; Wen et al., 2021). This phenomenon results in differences in water content at the same water potential and thus in water and air-filled pore connectivity between the drainage and the wetting branches of the soil water retention curve (Haines, 1930; Likos et al., 2014). Further, it explains the observations of Hamamoto et al. (2022) who reported differences in gas diffusion coefficients at the same air-filled porosity during a wetting–drying cycle.
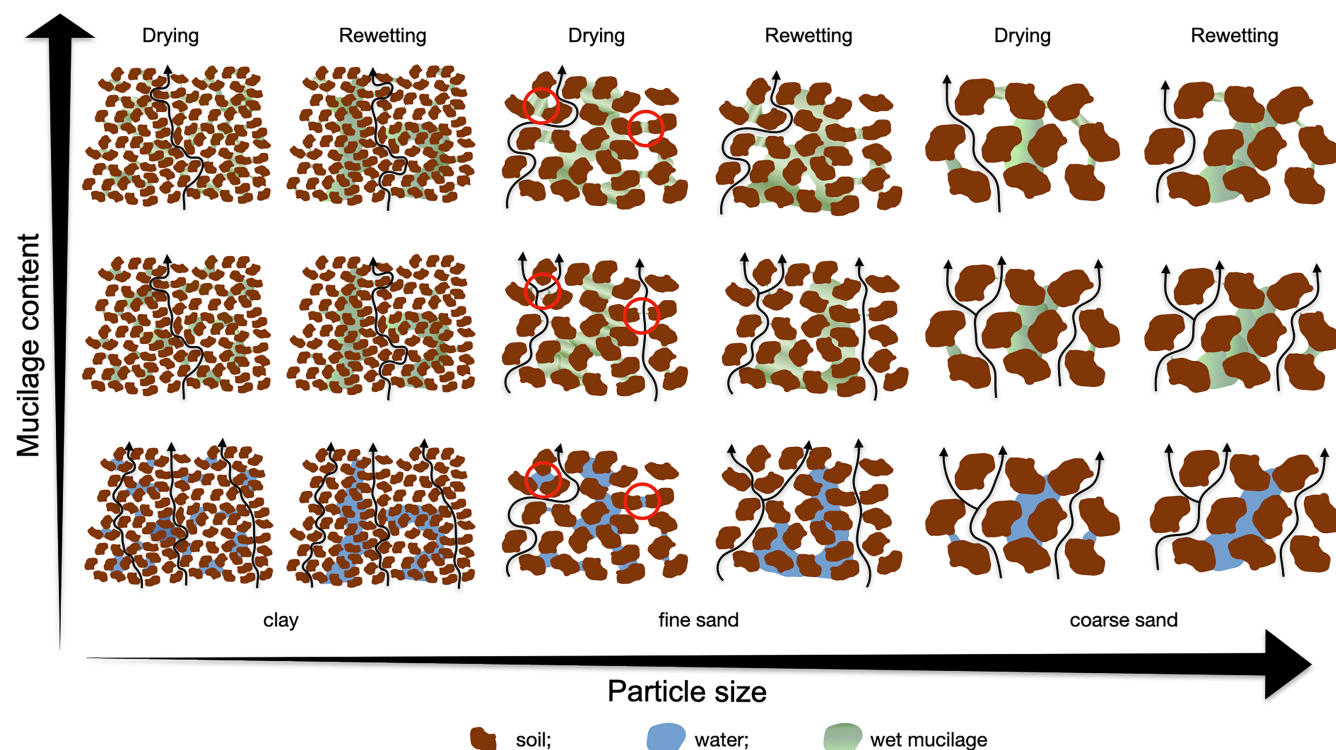
Plant roots actively modify the physical properties of the soil in their vicinity by secreting mucilage (Benard, Zarebanadkouki, Brax, et al., 2019; Carminati et al., 2016; Haupenthal et al., 2021; Kroener et al., 2018). Lazarovitch et al. (2018) stated that optimal plant growth requires a balance between water and O_2 contents. Mucilage may be a plant's tool to maintain this balance. The physico-chemical properties of root mucilage (e.g., water holding capacity, viscosity and surface tension) vary between plant species. Seed mucilage (e.g., from chia or flax seeds), which has physico-chemical properties similar to plant root mucilage, is often used as an analogue in experimental studies (Brax et al., 2020; Naveed et al., 2019). Studies have shown that mucilage has a strong impact on soil hydraulic properties (Benard, Zarebanadkouki, & Carminati, 2019; Carminati et al., 2010; Kroener et al., 2018), solute diffusion (Holz et al., 2019; Zarebanadkouki et al., 2019) and gas diffusion (Haupenthal et al., 2021) in soil. Due to its hydrogel-like behaviour, mucilage has the capacity to absorb water up to 600 times its own dry weight (Nazari, 2021). Furthermore, Benard et al. (2018) showed that the contact angle at the soil–water interface increased with mucilage content. Kroener et al. (2018) found that the effect of mucilage on saturated soil hydraulic conductivity and water retention depended on soil particle size. Mucilage reduced the hydraulic conductivity of fine sand by several orders of magnitude, whereas its effect was negligible in clay. Moreover, mucilage increased water content at low matric potentials in all soils. However, in coarse soils a comparably high mucilage content was needed to induce an increase in soil water retention.

The high viscosity of mucilage leads to the formation of characteristic bridges between soil particles during soil drying (Albalasmeh & Ghezzehei, 2014; Benard, Zarebanadkouki, & Carminati, 2019). Carminati et al. (2017), Benard et al. (2018), Haupenthal et al. (2021) and Esmaeelipoor Jahromi et al. (2022) observed various types of structures in different porous media. The shape of these bridges depends on mucilage content. Thin filaments are formed at low content. With increasing content, hollow cylinders were observed and at high mucilage content, 2D interconnected surfaces reaching through the pore space are formed. Benard et al. (2018) observed that for particles with a high surface roughness more mucilage is needed to create bridges similar sized compared to particles with a smooth surface. It is, therefore, reasonable to postulate that the interaction of mucilage with the soil matrix alters the connectivity of air-filled pores in soil.

Highlights

- Mucilage reduced gas diffusion in dry soils without affecting air-filled porosity.
- Effect of mucilage on soil gas diffusion is soil texture dependent.
- Gas diffusivity at the same water content was higher when soil was rewetted. The effect diminished with increasing mucilage content.
- CT imaging indicated improved connectivity of the gas phase at the same water content during soil rewetting.

FIGURE 1 Conceptual model of gas movement in soil as a function of mucilage content and particle size at a constant low water content. The distribution of water and mucilage depends on whether the soil is dried or rewetted. Mucilage content increases from left to right and particle size increases from bottom to top. Water and mucilage are clogging pores reducing gas diffusivity, indicated by extended diffusion pathways. Note that for fine sand swelling of mucilage displaces particles (red circles) without affecting porosity, resulting in large pores where mucilage at low contents is no longer able to span across a pore, leaving the pore open for gas to diffuse. This effect is neglected for clay since swollen mucilage would change the porosity of the soil, which would make the soil incomparable.

A conceptual model to describe the effect of mucilage on gas movement in soil under a drying–rewetting cycle for a given water content is shown in Figure 1. The shape of mucilage structures in soil and their effect on gas diffusion depends on mucilage content. An increase in mucilage content results in larger structures, hence a decrease in connectivity of air-filled pores, thereby limiting gas diffusion. The distribution of water in the pore space depends on whether the soil has been dried or rewetted. The main drivers for a different water distribution are air entrapment, an ink-bottle effect and a contact angle hysteresis (Diamantopoulos et al., 2013; Likos et al., 2014). In coarse soils with large average pore diameter the amount of potential pore throats is rather low. Therefore, not many bottleneck effects can be expected, resulting in a quite similar water distribution and consequently a comparable gas diffusivity between wetting and drying of the soil. With a decreasing particle size, the specific surface area of the particles increases and with it surface roughness, leading to a higher amount of potential pore throats. As a consequence, a bottleneck effect can occur more frequently. Therefore, a less connected air-filled porosity during drying compared to rewetting can be expected in fine soils. Hence, gas diffusion is higher during rewetting at the same water content. However, in clay the number of pores and potential pore throats is so high that water cannot be present in every pore throat during drying, therefore not affect air-filled pore connectivity and consequently gas diffusivity. In contact with water, mucilage starts to swell and expand throughout the pore space (Brax et al., 2017). As mucilage dries, persistent liquid bridges between particles can draw them together (Williams et al., 2021). Both processes can cause an alteration of the geometry of the soil by rearranging the particles and pores. In coarse soils with large pores, mucilage will swell into the pore space without affecting the pore structure. At low mucilage content, only a few mucilage bridges can be formed between soil particles, which do not affect gas diffusion. With increasing content, mucilage bridges will be able to span across larger pores (Carminati et al., 2017), disconnecting the gas phase and reducing gas diffusivity. Furthermore, mucilage is able to displace soil particles and change the structure of the soil (Hallett et al., 2022). In fine-textured soil, the swelling of mucilage results in the formation of large pores. During drying, water is no longer present within these large

pores, and at low mucilage content the pores are too wide for mucilage bridges to be formed. This process opens up pores for gas to diffuse through which increases diffusion. However, at high mucilage contents wider pores will be clogged again (Benard et al., 2021) and diffusivity decreases. In clay soils, swelling of mucilage is supposed to have the highest impact. Not only a change in soil structure is to be expected but also a change in total porosity, respectively bulk density, resulting in an increase in the soil volume (Kroener et al., 2018). For simplification, the effect of mucilage swelling in clay soils is neglected. Therefore, as with clay soil without mucilage, the gas diffusivity during drying and rewetting will not differ. Despite progress in conceptualizing the interactions between soil particles and mucilage, the impact of particle size and soil water content in the context of gas diffusion remains unclear.

The approach of using X-ray computed tomography (CT) to quantify soil structure has been established in recent years. It has been used in several studies for visualization and quantification of pore connectivity (Koestel et al., 2020; Lucas et al., 2021; Renard & Allard, 2013; Vogel, 1997), as well as pore alteration induced by roots (Aravena et al., 2011). Hamamoto et al. (2022) used X-ray CT to visualize differences in water distribution during a wetting–drying cycle. Common parameters to quantify the connectivity of the pore system are the Euler–Poincaré characteristic (EPC) χ and the Gamma (Γ-) indicator. Whilst χ describes the connectivity of the pore space characterized by its geometrical topology (Vogel, 1997), Γ represents the probability of finding a continuous path through the pore system (Lucas et al., 2021; Renard & Allard, 2013). Hence, the Γ-indicator is more sensitive to the global connectivity of the soil, whilst χ is independent of the size of pore clusters.

In this study, we investigated the effect of a root mucilage analogue on soil gas diffusion in the soil of different particle sizes and at different water contents for drying and rewetting conditions. Gas diffusion coefficients were determined experimentally at various mucilage contents during a drying–rewetting cycle. The experimental data were supported by X-ray CT and environmental scanning electron microscopy (ESEM) images. Our hypothesis was that the effect of mucilage on air-filled pore connectivity depends on particle size. We expected a substantial decrease in soil gas diffusivity with an increase in mucilage content as mucilage structures increase in size, thereby reducing the cross section of available pathways for gas diffusion. In coarse soils, a higher mucilage content would be required for structures to form which reach across big pores. In very fine-textured soils, we expected a reduced effect due to the number of potential pore throats where mucilage deposits and structures are formed during soil drying. In addition, we assumed a hysteresis in gas diffusion coefficient during a drying–rewetting cycle caused by the non-uniformity of interconnected pores. Finally, we hypothesized that the effect would diminish with increasing mucilage content as the structures formed during drying would attract water during rewetting and redistribute it to larger pores.

2 | MATERIALS AND METHODS

2.1 | Mucilage collection

Chia seed mucilage was used as an analogue for root mucilage. A detailed description of the extraction process is given by Kroener et al. (2018). After the extraction, mucilage was frozen, then freeze-dried and ball-milled.

2.2 | Gas diffusion measurements

The experimental setup was based on a diffusion chamber method, described in detail by Haupenthal et al. (2021) (Figure 2). It was modified to reduce leakage by removing the gas inlet and outlet, and the chamber was vented through the opening in the sample holder frame before the measurement. Furthermore, the sample holder was fixed to avoid vibrations induced by air turbulence whilst sliding the sample holder over the opening.
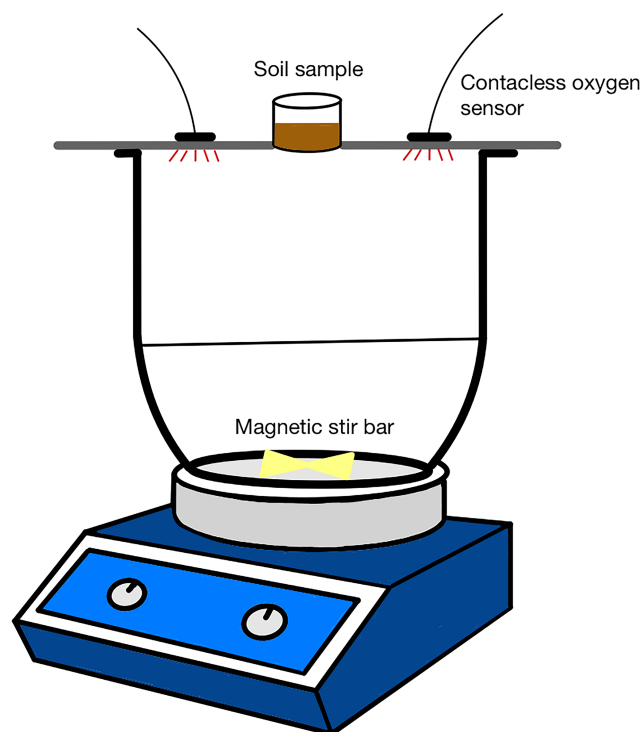
**FIGURE 2** Experimental setup for gas diffusion measurements based on the diffusion chamber method.

Therefore, initially sealed samples were placed on the sample holder and opened to start the measurement. In addition, contactless O_2 sensors (Pyroscience GmbH, Aachen, Germany) were used. Gas diffusion coefficient (D_p/D_0) was measured during a drying–rewetting cycle. Oxygen was used as a tracer gas. The diffusion coefficient of O_2 in air (D_0) at 20°C and 1013 hPa is 0.231 cm^2 s^{-1} (Wiegleb, 2016). A soil–mucilage mixture was used as a model of the rhizosphere. We mixed soils of various particle sizes (800–1000, 500–800, 200–500, 63–200, 20–63 μm and <20 μm) with different amounts of chia seed mucilage to achieve specific mucilage content in soil (0, 0.5, 1, 2.5, and 5 mg g^{-1} dry mucilage/dry soil). Coarse sandy soil (800–1000 and 500–800 μm, Quarzwerk WOLFF & MÜLLER, Haida, Germany), medium and fine sand, silty and clay soil (Quarzwerke Frechen, Frechen, Germany; organic matter content below detection limit) were used. Three replicates of each combination of particle size and mucilage content were prepared at a dry bulk density of 1.51 ± 0.05 g cm^{-3}. Soil–mucilage mixtures were packed in PVC tubes with a diameter of 3.6 cm and a height of 0.6 ± 0.01 cm. Air-filled porosity was derived from bulk density, particle density (2.65 g cm^{-3}) and volumetric water content, and ranged from 0.43 ± 0.015 cm^3 cm^{-3} (total porosity) for dry samples to 0.23 ± 0.015 cm^3 cm^{-3} for the highest water content. Mucilage was diluted in water. The amount of water for dilution was determined by setting the volumetric water content (Φ_V) equal to the porosity of the sample. Thereby, saturating the sample but not exceeding soil porosity. Silt and clay samples were slightly compacted during the drying process using a stamp to counteract the swelling of the samples and maintain the original soil volume. Samples were air-dried (22 ± 1°C) and the weight was monitored to determine gravimetric and volumetric water content, seeking Φ_V of 0.1, 0.15 and 0.2 cm^3 cm^{-3} for testing. For rewetting, the amount of water corresponding to the pre-defined Φ_V was applied by drip irrigation using a pipette. Before measurements, the samples were closed with parafilm (Amcor, Zurich, Switzerland) and stored at 4°C for at least 4 h to ensure equilibration of the water content across depth whilst limiting microbial activity. During drying, the evaporation rate was monitored. To maintain the desired water content during diffusion measurements, water was resupplied to the soil surface every 30 min based on the recorded evaporative loss. The measurements were performed at room temperature (22 ± 1°C).

2.3 | X-ray CT-imaging

Sand (Carlo Bernasconi AG, Zurich, Switzerland) was sieved (200–500 μm) and mixed with wet mucilage to achieve a range of mucilage content in soil (0, 1 and 2.5 mg g^{-1}), and air-dried, respectively wetted via capillary rise, to Φ_V of 0.1 0.15 and 0.2 cm^3 cm^{-3}. Sample holders were sealed with parafilm to avoid evaporative losses and stored at 4°C for 4 h to reach equilibrium in matric potential before imaging. Immediately after rewetting and sealing the samples, additional CT scans were performed. X-ray CT images were taken with a GE Phoenix V|tome|x s micro-CT scanner (General Electric Company, Boston, MA, United States) with a tube voltage of 140 kV and a tube current of 70 μA. An actual pixel size of 11×11 μm^2 was achieved at a scan time of 17 min. Images were reconstructed from 2000 projections using the Phoenix datos|x CT Data Acquisition Software. Reconstructed images (consisting of 1012 slices) were analysed using the analysis software Avizo (Thermo Fisher Scientific, Waltham, MA, USA). For preprocessing, the following steps in corresponding order were performed: (i) Since concave and convex deformations occurred at the top and bottom of the samples, respectively, during sample preparation, the total number of slices was reduced to 700 during image preprocessing, removing the upper- and lowermost layers from the processed image. This resulted in a consistent cylindrical shape of the CT images, allowing for accurate comparisons of the different treatments, but also in minor changes in water content calculated from the CT image analysis. (ii) Images were converted from 16 to 8 bit and, to reduce noise, a non-local means as well as an unsharp masking filter were applied. (iii) The diameter of the sample holder was 1 cm; images were cut cylindrically with a diameter of 0.89 cm to match the sample geometry and to minimize edge effects at the cylinder wall. (iv) A grey-scale value histogram was created to determine the markers of the solid, liquid and gaseous phases, which were required as input for the watershed transformation. Therefore, a rolling window calculation was applied at each greyscale with a centre labelled window of size 5 to determine the mean of the values within the window. This resulted in a smooth curve over the data, which was then used to find the peak values, corresponding to each phase. To have a standardized procedure, the interval of grey-scale values defining each phase was evaluated at a relative height of 0.5 between the height of the peak itself and the lowest contour line. At this height, the width of the curve determines the threshold values for the respective phase. (v) Afterwards, markers derived from the histogram analysis were used as input for a marker-based watershed transformation (Beucher & Meyer, 1993) to segment the different phases (soil, water and air). (vi) Finally, a morphological opening with a sphere of radius 2 px as the structuring element was applied to account for features with a volume below the spatial
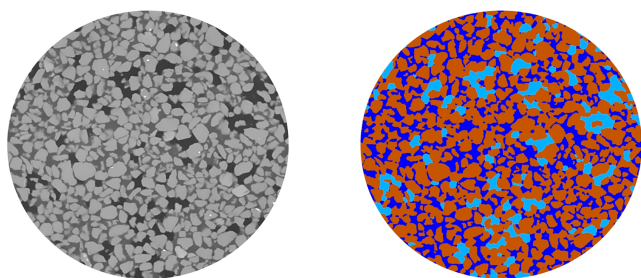
FIGURE 3 Exemplary cross section of a raw and corresponding segmented x-ray CT image with water (dark blue), air (light blue) and soil (brown).

resolution limit. An exemplary cross section of the segmented result is shown in Figure 3.

The connectivity of the gas phase was estimated based on the EPC χ and the Γ-indicator. Calculation of χ was done by applying a label analysis based on the Avizo inbuilt EPC measure using a 26-neighbourhood algorithm. χ is related to the topology of the pore space, dimensionless, and is based on the number of unconnected clusters (N), the number of redundant connections (C) and number of completely enclosed cavities (H) (Vogel, 2002):

$$\chi = N - C + H. \qquad (1)$$

For a network of pores in soil, H is negligible (Vogel, 2002). The larger the χ, the lower is the connectivity of the pore system. Typically, χ is highly negative in soils, indicating a high connectivity of the pore space. However, a negative χ does not imply the presence of a percolating path connecting the top and bottom of a soil sample (Lucas et al., 2021).

Another metric to describe pore connectivity is the Γ-indicator. The Γ-indicator is a measure of probability for two voxels belonging to the same cluster, and consequently being connected. For soil–water–air samples it can be calculated from the total number of all air-filled pore voxels ($N_{p_{air}}$), the number of all air clusters k_{air} ($N_{k_{air}}$) and the number of air-filled pore voxels p_{air} contained in each cluster k_{air} ($n_{p_{k_{air}}}$). $\Gamma(p_{air})$ is defined as (Renard & Allard, 2013):

$$\Gamma(p_{air}) = \begin{cases} \dfrac{1}{N_{p_{air}}^2} \sum_{k=1}^{N_{k_{air}}} n_{p_{k_{air}}}^2 & p_{air} \neq 0 \\ 0 & p_{air} = 0 \end{cases}. \qquad (2)$$

A Γ value of one indicates that all air-filled pore voxels are connected and consequently belong to the same, single cluster. In contrast, a value close to zero indicates the presence of many unconnected air-filled pore clusters.

However, both measures do not provide information on the volume of the connected pore clusters and whether there is a percolating path from the bottom to the top of the sample (Koestel et al., 2020).

2.4 | Environmental scanning electron microscopy

Samples packed with the same soil textures and mucilage contents as for diffusion measurements were scanned using ESEM. Samples were dried for 48 h at room temperature ($22 \pm 1°C$). Prior to the measurements, samples were coated with gold using a Quorum Q 150R S Rotary Pumped Coater (Quorum Technologies, Judges House, Lewes Road, Laughton, East Sussex, UK). ESEM images were taken with an FEI Quanta 250 ESEM (FEI Company, Hillsboro, OR, United States) under low vacuum with chamber pressures between 60 and 80 Pa. A large field detector was used with an acceleration voltage of 30 kV.
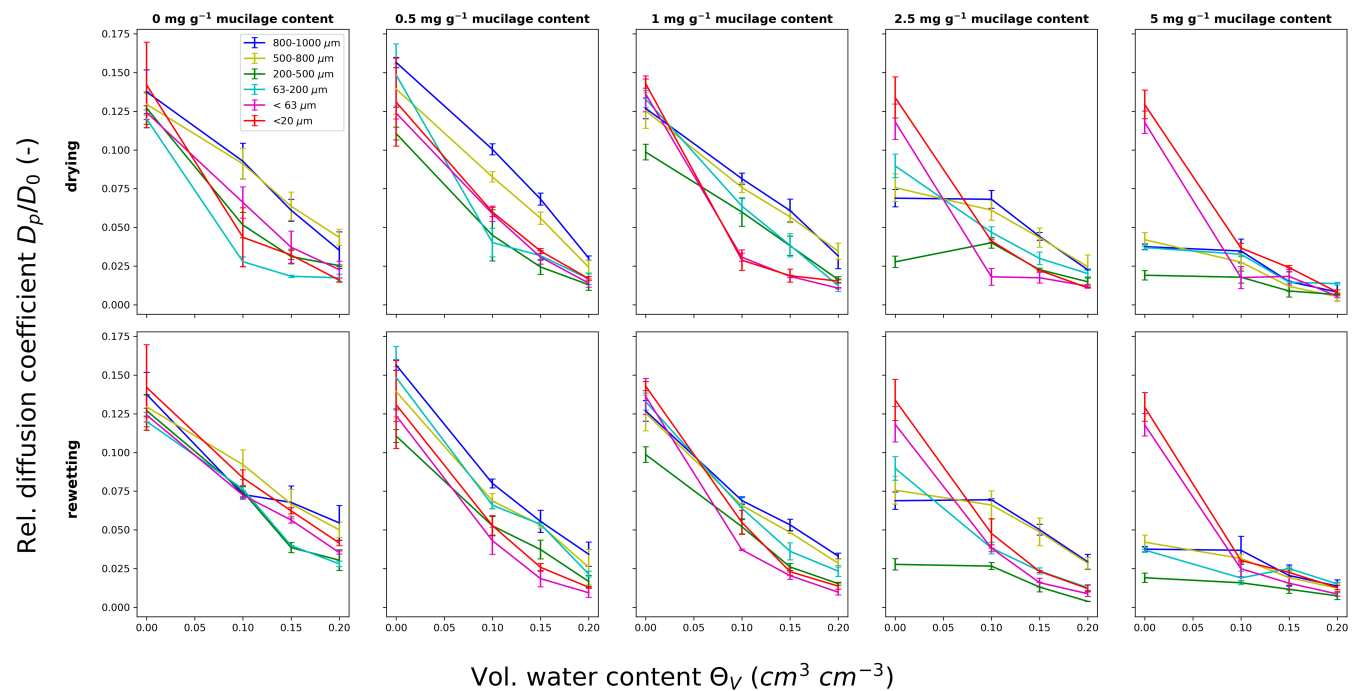
3 | RESULTS

3.1 | Gas diffusion measurements

The amount of mucilage per sample ranged from 0.495 to 5.1 mg g^{-1} dry mucilage/dry soil, depending on initial mucilage content. Assuming a mucilage density of roughly 1 g cm^{-3}, the volumetric mucilage fraction would be roughly 0.9%. Thus, the volume occupied by pure mucilage would be <1% of the volume of the bulk soil. Therefore, the effect of dry mucilage on air-filled porosity was assumed negligible.

In Figure 4, the relative diffusion coefficient D_p/D_0 is plotted as a function of water content for various particle sizes and mucilage content during a drying–rewetting cycle. A comprehensive presentation of the results differentiated by mucilage content and particle size can be found in the supplemental material (Figure S1). Generally, D_p/D_0 decreased with increasing water content and increasing mucilage content (Table 1). The effect of mucilage on gas diffusion was highly dependent on the particle size. The reduction in medium sandy soil (200–500 μm) was six times larger than the reduction in silty and clay soil.

For untreated samples, a hysteresis in D_p/D_0 during the drying–rewetting cycle was observed. The extent of the hysteresis depended on particle size. Whilst the coarse soils showed no difference, D_p/D_0 was significantly lower during drying in fine soils. This effect

FIGURE 4 Relative diffusion coefficient D_p/D_0 depending on water content and mucilage content during drying (top row) and rewetting (bottom row). Results indicate a hysteresis for control treatments which diminished with an increase in mucilage content.

TABLE 1 Relative diffusion coefficient (D_p/D_0) for dry samples without mucilage and the reduction of D_p/D_0 caused by mucilage and water.

Parameter	Particle size					
	1000–800 μm	500–800 μm	200–500 μm	63–200 μm	<40 μm	<20 μm
D_p/D_0 for control soil	0.137	0.129	0.127	0.12	0.124	0.142
Reduction factor caused by mucilage (5 mg g^{-1})	3.66	3.08	6.68	4.24	1.01	1.08
Reduction factor caused by water (0.2 cm^3 cm^{-3} drying)	3.91	2.93	5.08	6.9	5.39	8.88
Reduction factor caused by water (0.2 cm^3 cm^{-3} rewetting)	2.49	2.58	4.23	4.29	3.54	3.38

Note: The reduction caused by mucilage was highest for 200–500 μm particle size. For silt (<40 μm) and clay (<20 μm) no reduction could be observed. The reduction caused by water was higher during drying compared to rewetting.

diminished with increasing mucilage content. At the highest water content (20%), diffusivity changed only slightly with increasing mucilage content.

3.2 | X-ray CT-imaging

The EPC χ for the gas phase decreased for all mucilage contents with decreasing water content, whilst for the liquid phase χ decreased for increasing water content for all mucilage contents (Figure 5). Φ_V values were lower than initially set due to image processing, during which the

top and bottom of the image stack were cut off. Due to drying from evaporation and wetting from the capillary rise, more volume of water than volume of air was removed. This resulted in a reduced calculated soil moisture content. Results for samples without mucilage indicated a hysteresis behaviour for the gas phase. Values for χ during rewetting were slightly smaller compared to drying for water contents above 10%. With the addition of mucilage, the hysteresis diminished. However, for the liquid phase no differences in χ during drying and rewetting, and consequently no hysteresis was observed for all mucilage contents.
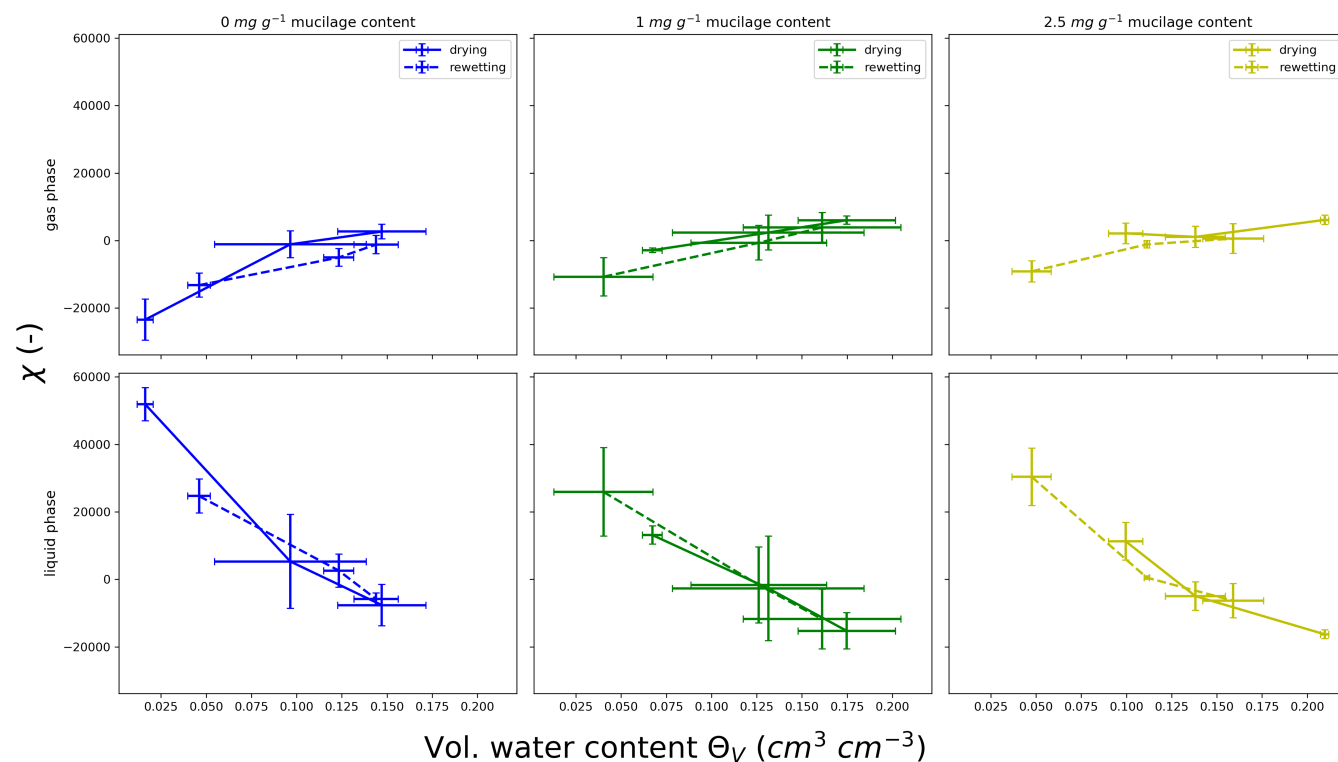
FIGURE 5 Euler–Poincaré characteristic χ for the gas (top) and liquid phase (bottom) depending on water content and mucilage content.
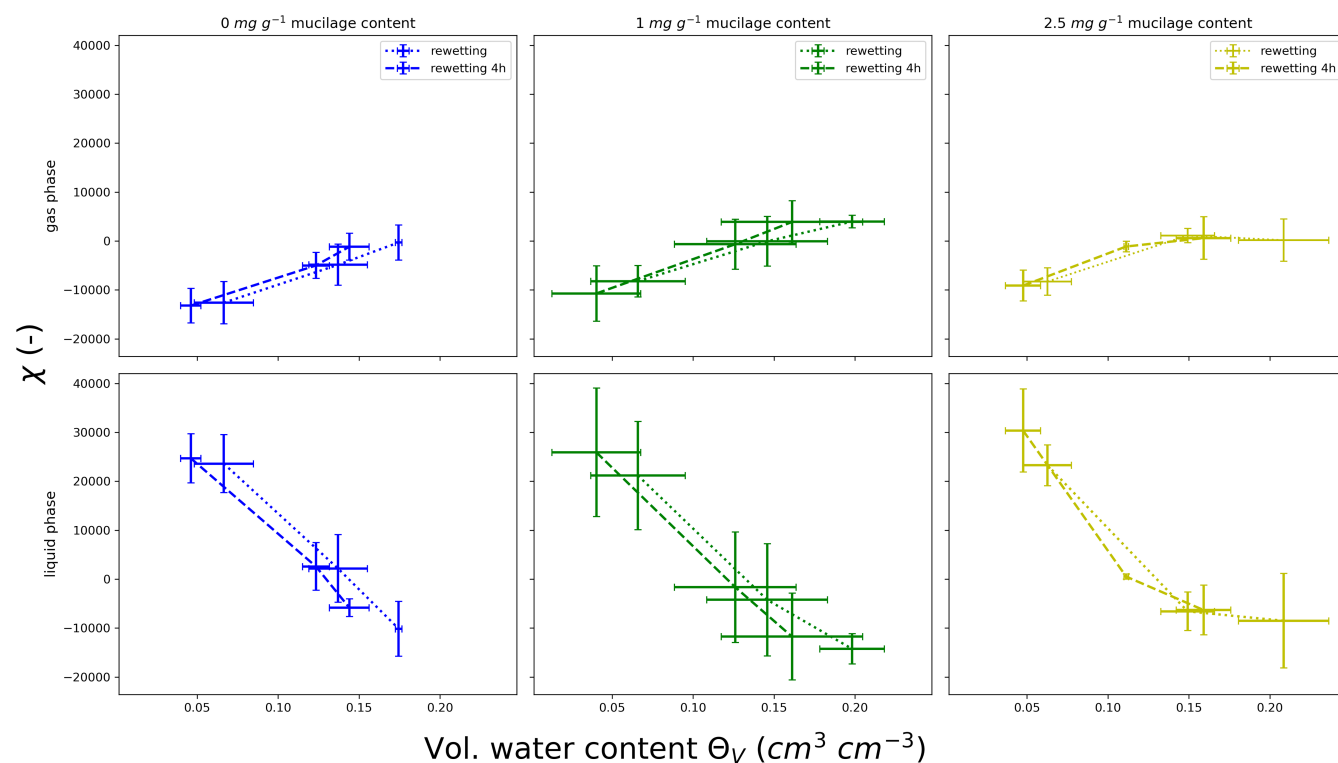
FIGURE 6 Euler–Poincaré characteristic χ immediately after rewetting and 4 h after rewetting. The connectivity of the liquid phase improved over time whilst the connectivity of the gas phase decreased. The effect seems to diminish with increasing mucilage content.
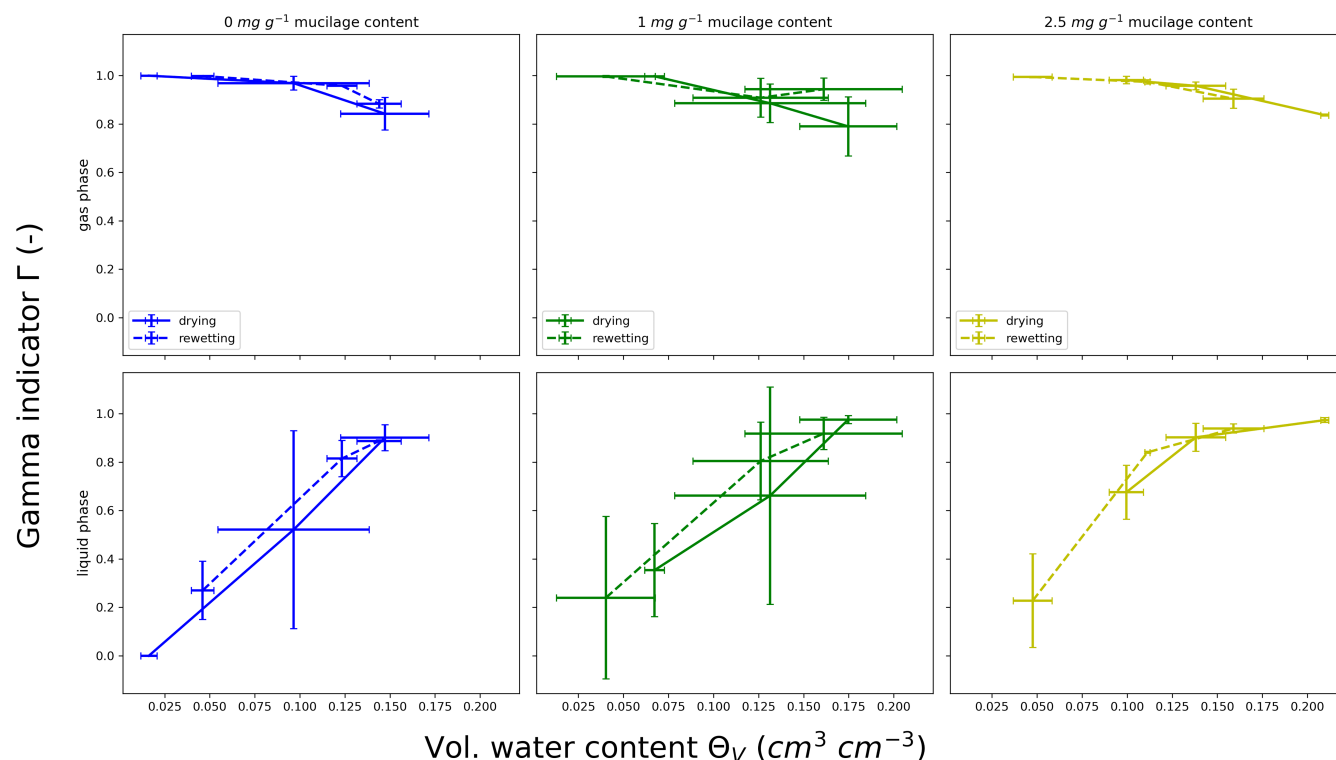
FIGURE 7 Gamma indicator for the gas and liquid phase depending on water content and mucilage content.

Results for χ immediately after rewetting and after 4 h showed no significant differences, indicating that the topology of the air–water–mucilage phase equilibrates quickly (Figure 6).

The Γ-indicator of the gas phase decreased with increasing water content in all treatments (Figure 7). In contrast to diffusion coefficient measurements, no significant difference between drying and rewetting could be observed. Overall, values for all mucilage contents were in the same range as their corresponding water content. For the liquid phase, values increased with increasing water content. Values for various mucilage contents did not differ significantly. Also, no major differences between drying and rewetting could be observed. Furthermore, values immediately after rewetting and after 4 h showed no significant difference (Figure 8). As with the EPC, this showed a quick equilibration of the air–water–mucilage phase.

Comparison of the percolating gas phase cluster for various mucilage and water contents indicates a reduction of the connectivity throughout the sample with increasing mucilage and water content (Figure S1).

3.3 | Environmental scanning electron microscopy

The ESEM images reveal various dried mucilage structures in the dried soil samples depending on mucilage content. These structures ranged from thin filaments at low mucilage content, membrane-like structures and hollow cylinders at intermediate content up to interconnected surfaces spanning throughout the pore space at high content (Figure 9). Whilst at low content, mucilage deposits preferentially in pores with small diameters, mucilage bridges span across larger pores with increasing content. However, even at low content interconnected surfaces were observed, whilst with increasing content the size of these surfaces increased.

4 | DISCUSSION

The gas diffusion measurements of soils with various particle sizes and mucilage content under a drying–rewetting cycle supports the conceptual model (Figure 1). In dry soils, the effect of mucilage on gas diffusion depends on soil texture and mucilage content (Figure 4). At low mucilage contents (0.5–1 mg g^{-1}), only a minor reduction in D_p/D_0 could be observed. With mucilage content increasing (2.5–5 mg g^{-1}), gas diffusivity was reduced for the coarse, medium and fine sandy soils, whilst for silt and clay no reduction could be observed. In general, when mucilage caused a reduction of D_p/D_0 in dry soils, it did not affect air-filled porosity. At the same water content, the diffusivity differed between dried and rewetted soils. However, the diffusion always depended on mucilage
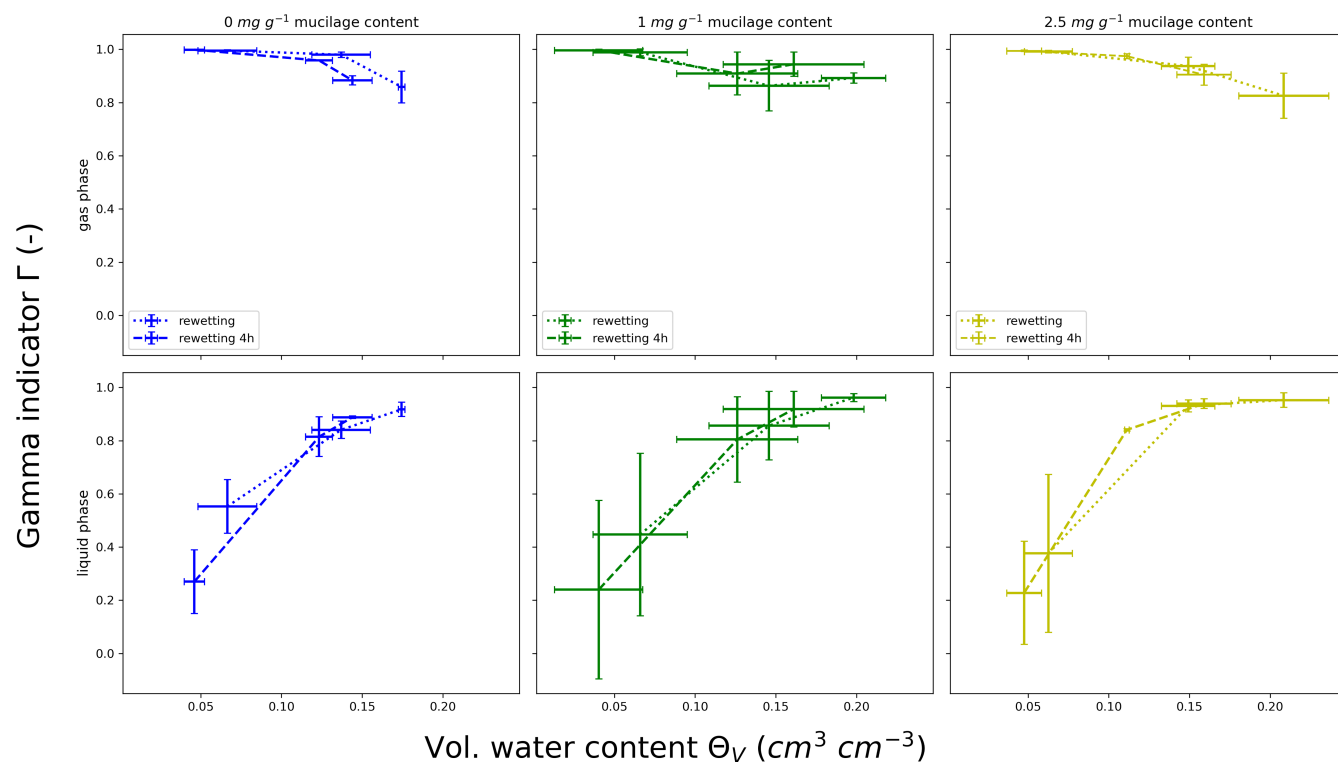
FIGURE 8 Gamma indicator for the gas and liquid phase depending on water content and mucilage content immediately after rewetting and 4 h after rewetting.
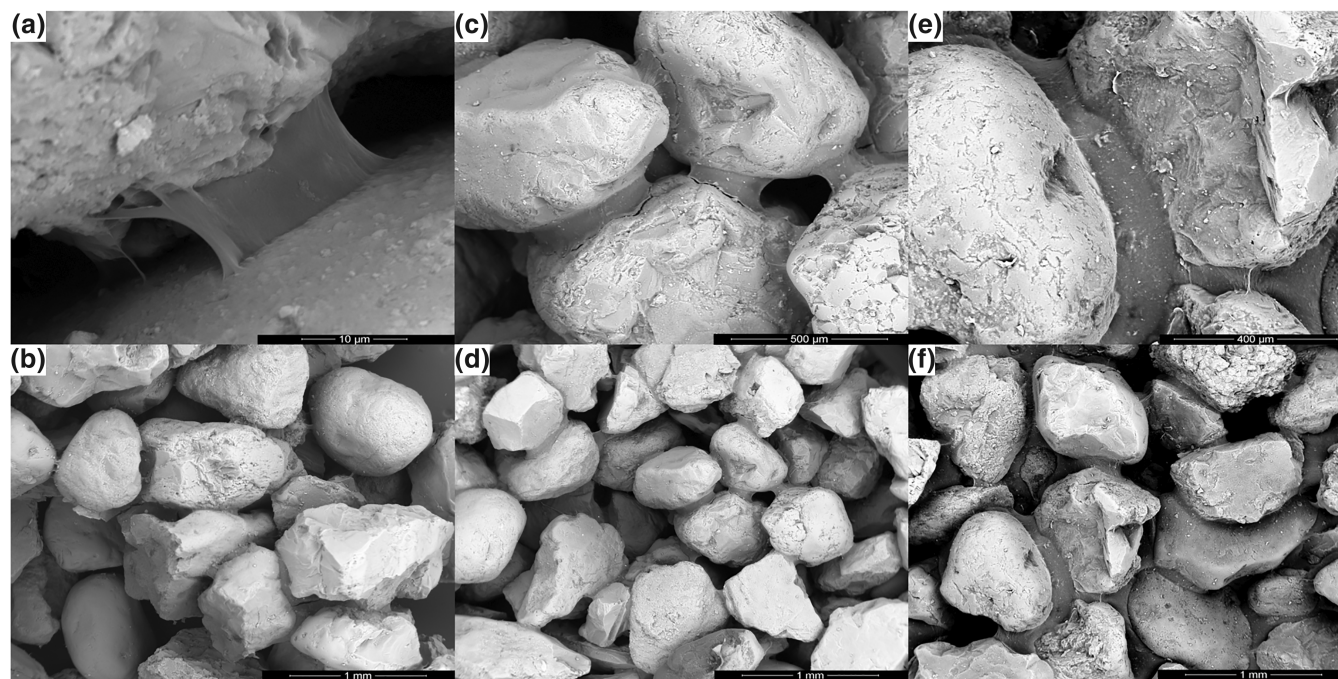
FIGURE 9 ESEM images of mucilage deposits in the pore space of coarse sandy soil with 500–800 μm, respectively 800–1000 μm particle size. Mucilage content increases from left to right (a, b 1 mg g^{-1}, c, d 2.5 mg g^{-1}, e, f 5 mg g^{-1}). Various mucilage concentration-dependent structures are visible in the images: (a, b) Thin filaments and membrane-like structures are dominant, but also small connected surfaces are visible. (c, d) Cylindrical structures became visible with increasing mucilage content. (e, f) At the highest content, interconnected surfaces span across multiple pores.

content (Figure 4). Thorbjørn et al. (2008) proposed a conceptual model in which gas diffusivity depends on particle size. However, no significant differences in diffusion coefficient depending on particle size for dry samples without mucilage could be observed in our study (Table 1). All samples were prepared to have the same bulk density. Furthermore, the density of the soil particles was the same, thus air-filled porosity was the same between the differently textured soils. Liu et al. (2006) reported that for an artificial macropore network (pores smaller than ∼100 μm are assumed to be blocked) no universal relationship between diffusion coefficient and porosity exists. Local porosity heterogeneities could lead to deviations in gas diffusivity. Furthermore, tortuosity is related to the weighted length of diffusion pathways. The soil samples used in this study were very thin (0.6 cm), consequently, the effect of porosity fluctuations and tortuosity can be assumed negligible, which could explain the similar gas diffusivity for all textures. The driest samples showed the biggest reduction in D_p/D_0 for medium sandy soil mixed with mucilage compared to the untreated medium sand samples. At $0\,\mathrm{cm}^3\,\mathrm{cm}^{-3}$ water content and mucilage content of $2.5\,\mathrm{mg\,g}^{-1}$, the diffusion coefficient of the untreated samples was reduced by a factor of 5 and increased to a factor of 6.68 for $5\,\mathrm{mg\,g}^{-1}$ (Table 1). Mucilage structures observed via ESEM seem to disconnect the gas phase significantly, and the ratio between pore size and the amount of potential pore throats seems to be optimal in medium sand (200–500 μm) for mucilage to span across many pores and have a significant effect on gas diffusivity. In coarse sandy soil (500–800 and 800–1000 μm) and fine sandy soil (63–200 μm) the effect is smaller. In coarse soil, the average pore seems to be too large for mucilage to span across, whilst in fine sand, and even more so in silty and clayey soil, the number of potential pore throats was higher, and mucilage would not be present in every pore. Therefore, mucilage likely accumulates in certain regions of the pore space, leaving others available for gas diffusion. Furthermore, the higher surface roughness of silt and clay particles compared to sand might lead to more, but smaller mucilage structures as observed by Benard et al. (2018). As a result, no reduction in gas diffusivity could be observed for silt and clay. A similar particle size-dependent effect was observed by Kroener et al. (2018), where mucilage had no effect on the saturated hydraulic conductivity of clay soil. Note that since the physicochemical properties differ amongst mucilage from different plants and environmental conditions, it is reasonable to assume that their effect on gas diffusion is also variable.

Furthermore, our results confirm the findings of Hamamoto et al. (2022), who also observed a hysteresis in the gas diffusion coefficient during a drying–rewetting cycle. The hysteresis was more distinct in fine soils. These observations are in good agreement with the concept of an ink bottle, small bottle throat diameter and broad bottle body diameter, caused by the non-uniformity of interconnected pores, as well as the concept of differences in solid–liquid contact angles during wetting and drying (Haines, 1930; Likos et al., 2014). During drying, narrow parts of interconnected pores are able to hold water and increase the length of diffusion pathways. During rewetting, water might not reach the narrow parts of the pore, leaving space for gas to diffuse. Additionally, lower contact angles between the soil and water during drying lead to less connected air-filled pores resulting in a lower gas diffusivity. However, if mucilage is added this effect diminishes with increasing mucilage content. With mucilage, liquid bridges persist under drying. As they dry further, they are likely to draw particles together, enhancing local soil aggregation (Williams et al., 2021). As mucilage rewets, it starts to absorb water and swells. Both processes are likely to create preferential diffusion pathways, increasing gas diffusivity and reducing the hysteresis effect. Despite this, mucilage can increase the contact angle at the soil–water interface, especially under dry conditions (Benard et al., 2018). This results in more similar water–soil contact angles during drying and wetting, reducing the hysteresis effect in the water retention, and consequently leading to a diminishing hysteresis in gas diffusivity during a drying–rewetting cycle. In our conceptual model for fine sand, the ability of mucilage to absorb large amounts of water and swell can cause an alteration of the soil structure. Swelling mucilage exerts stress on soil particles. Changes in soil structure were reported in studies with super-absorbing polymers mixed with soil (Misiewicz et al., 2020; Saha et al., 2022). Results for D_p/D_0 in medium (200–500) and fine soil (63–200) showed a distinct increase in gas diffusion at low mucilage content during drying compared to untreated samples. Swollen mucilage created larger pores by displacing soil particles. With increasing diameter, the capillary forces in the pore decrease and water can no longer be retained. At the same time as the soil dries, mucilage at low contents can no longer bridge the enlarged pores, and gas can now diffuse through the pore. A similar effect can be expected when drying liquid bridges draw particles together. However, at high mucilage contents, D_p/D_0 decreased in both scenarios, that is, drying and rewetting. At increasing content, mucilage can extend even across larger pores, and diffusion pathways are blocked again. Furthermore, connected mucilage bridges that were formed during drying turn hydrophilic after some time (Zickenrott et al., 2016) and draw water during rewetting to areas that otherwise would not have been reached by water. Results for coarse sand indicate no distinct change in soil structure. Large particles might

be too heavy to be displaced by the mucilage, instead mucilage tends to swell into empty pore space during wetting or liquid bridges break during drying. In the experiments, a visible swelling of the silt and clay soil samples was observed. Since the swelling mucilage caused an increase in the height of the samples, we suppressed that effect to maintain soil porosity. Therefore, D_p/D_0 decreased in both cases even at low mucilage contents.

The EPC χ and the Γ-indicator revealed a better-connected gas phase at low water contents and an increased liquid phase connectivity with increasing water content. Whilst χ values of the gas phase for samples without mucilage were higher for rewetted samples compared to dried samples, the effect diminished for the samples with mucilage. The variations in water distribution between drying and rewetting led to a hysteresis effect in the connectivity of the gas phase. This hysteresis during a drying–rewetting cycle, as well as its reduction with increasing mucilage content, was in good agreement with results from gas diffusion measurements (Figure 4), where diffusivity was higher during rewetting for samples without mucilage. However, the hysteresis was not as distinct as expected based on gas diffusion measurements. Furthermore, dry mucilage can be temporarily water repellent (Moradi et al., 2012; Zickenrott et al., 2016). Therefore, it is expected that immediately after rewetting, water preferentially saturates pores that are unaffected by mucilage, additionally disconnecting the gas phase. As a result, a less connected gas phase compared to a state when mucilage has turned hydrophilic and absorbed the water is likely. However, in our study χ and Γ measurements showed no such differences. This might be a consequence of the limitation in spatial and temporal image resolution, due to which it was not possible to detect mucilage directly. As a consequence, mucilage structures (Figure 9), which may have disconnected the gas phase, could not be explicitly considered resulting in an overestimation of the connectivity of the gas phase in treated soils. Furthermore, parts from the top and bottom of the image stack of each sample were removed during image processing. This altered the soil moisture content, which may have also impacted the connectivity of the liquid and gaseous phases.

5 | CONCLUSION

This study showed that the effects of mucilage on soil gas diffusion processes at the pore scale depended on basic physical soil properties. It indicates that by secreting mucilage from roots, plants can help mitigate changes in gas diffusivity induced by soil moisture fluctuations. Results show that dry mucilage reduced soil gas diffusion without affecting air-filled porosity. The effect of mucilage on soil diffusivity depended highly on particle size and mucilage content. Whilst the biggest effect could be observed in medium sand, no differences were observed in silt and clay soils. During a drying–rewetting cycle, hysteresis in the gas diffusion coefficient and gas phase connectivity could be observed in samples without mucilage. With increasing mucilage content this effect diminished. Results indicate that swelling mucilage can alter the structure of the soil, especially in soils with fine particles. Yet, a quantitative description of the influence of mucilage on soil structure is missing. This study supports the hypothesis that plants actively try to maintain stable physical conditions in the soil around the root and that they balance oxygen and water content by secreting mucilage.

CONFLICT OF INTEREST STATEMENT

The authors declare no conflict of interest.

DATA AVAILABILITY STATEMENT

The data that support the findings of this study are available from the corresponding author upon reasonable request.

ORCID

Adrian Haupenthal https://orcid.org/0000-0002-9165-3378
Pascal Benard https://orcid.org/0000-0002-0922-5527
Hermann F. Jungkunst https://orcid.org/0000-0002-9807-9401
Eva Kroener https://orcid.org/0000-0002-4732-3486
Nicolas Brüggemann https://orcid.org/0000-0003-3851-2418

REFERENCES

Albalasmeh, A. A., & Ghezzehei, T. A. (2014). Interplay between soil drying and root exudation in rhizosheath development. *Plant and Soil*, 374(1), 739–751. https://doi.org/10.1007/s11104-013-1910-y

Aravena, J. E., Berli, M., Ghezzehei, T. A., & Tyler, S. W. (2011). Effects of root-induced compaction on rhizosphere hydraulic properties - X-ray microtomography imaging and numerical simulations. *Environmental Science & Technology*, 45(2), 425–431. https://doi.org/10.1021/es102566j

Benard, P., Zarebanadkouki, M., Brax, M., Kaltenbach, R., Jerjen, I., Marone, F., Couradeau, E., Felde, V. J. M. N. L., Kaestner, A., & Carminati, A. (2019). Microhydrological niches in soils: How mucilage and EPS alter the biophysical properties of the rhizosphere and other biological hotspots. *Vadose Zone Journal*, 18(1), 180211. https://doi.org/10.2136/vzj2018.12.0211

Benard, P., Zarebanadkouki, M., & Carminati, A. (2019). Physics and hydraulics of the rhizosphere network. *Journal of Plant Nutrition and Soil Science*, 182(1), 5–8. https://doi.org/10.1002/jpln.201800042

Benard, P., Zarebanadkouki, M., Hedwig, C., Holz, M., Ahmed, M. A., & Carminati, A. (2018). Pore-scale distribution of mucilage affecting water repellency in the rhizosphere. *Vadose Zone Journal*, 17(1), 170013. https://doi.org/10.2136/vzj2017.01.0013

Benard, P., Schepers, J. R., Crosta, M., Zarebanadkouki, M., & Carminati, A. (2021). Physics of viscous bridges in soil biological hotspots. *Water Resources Research*, 57(11), e2021WR030052.

Beucher, S., & Meyer, F. (1993). *The morphological approach to segmentation: The watershed transformation, mathematical morphology in image processing* (pp. 433–481). Marcel Dekker Inc.

Brax, M., Buchmann, C., Kenngott, K., Schaumann, G. E., & Diehl, D. (2020). Influence of the physico-chemical properties of root mucilage and model substances on the microstructural stability of sand. *Biogeochemistry*, 147(1), 35–52. https://doi.org/10.1007/s10533-019-00626-w

Brax, M., Buchmann, C., & Schaumann, G. E. (2017). Biohydrogel induced soil–water interactions: How to untangle the gel effect? A review. *Journal of Plant Nutrition and Soil Science*, 180(2), 121–141.

Carminati, A., Benard, P., Ahmed, M. A., & Zarebanadkouki, M. (2017). Liquid bridges at the root-soil interface. *Plant and Soil*, 417(1), 1–15. https://doi.org/10.1007/s11104-017-3227-8

Carminati, A., Moradi, A. B., Vetterlein, D., Vontobel, P., Lehmann, E., Weller, U., Vogel, H.-J., & Oswald, S. E. (2010). Dynamics of soil water content in the rhizosphere. *Plant and Soil*, 332(1), 163–176. https://doi.org/10.1007/s11104-010-0283-8

Carminati, A., Zarebanadkouki, M., Kroener, E., Ahmed, M. A., & Holz, M. (2016). Biophysical rhizosphere processes affecting root water uptake. *Ann Bot*, 118(4), 561–571. https://doi.org/10.1093/aob/mcw113

Cooper, L. J., Daly, K. R., Hallett, P. D., Naveed, M., Koebernick, N., Bengough, A. G., George, T. S., & Roose, T. (2017). Fluid flow in porous media using image-based modelling to parametrize Richards' equation. *Proceedings of the Royal Society A: Mathematical, Physical and Engineering Sciences*, 473(2207), 20170178.

Diamantopoulos, E., Durner, W., Reszkowska, A., & Bachmann, J. (2013). Effect of soil water repellency on soil hydraulic properties estimated under dynamic conditions. *Journal of Hydrology*, 486, 175–186.

Esmaeelipoor Jahromi, O., Knott, M., Mysore Janakiram, R. K., Rahim, R., & Kroener, E. (2022). Pore-scale simulation of mucilage drainage. *Vadose Zone Journal*, 21(5), e20218. https://doi.org/10.1002/vzj2.20218

Fujikawa, T., & Miyazaki, T. (2005). Effects of bulk density and soil type on the gas diffusion coefficient in repacked and undisturbed soils. *Soil Science*, 170, 892–901. https://doi.org/10.1097/01.ss.0000196771.53574.79

Gardner, C. M., Laryea, K. B., & Unger, P. W. (1999). *Soil physical constraints to plant growth and crop production* (Vol. 11). Land and Water Development Division, Food and Agriculture Organization.

Gliński, J., & Stępniewski, W. (1985). *Soil aeration and its role for plants*. CRC Press.

Haines, W. B. (1930). Studies in the physical properties of soil. V. The hysteresis effect in capillary properties, and the modes of moisture distribution associated therewith. *The Journal of Agricultural Science*, 20(1), 97–116. https://doi.org/10.1017/S002185960008864X

Hallett, P. D., Marin, M., Bending, G. D., George, T. S., Collins, C. D., & Otten, W. (2022). Building soil sustainability from root–soil interface traits. *Trends in Plant Science*, 27(7), 688–698.

Hamamoto, S., Moldrup, P., Kawamoto, K., & Komatsu, T. (2009). Effect of particle size and soil compaction on gas transport parameters in variably saturated, sandy soils. *Vadose Zone Journal*, 8(4), 986–995. https://doi.org/10.2136/vzj2008.0157

Hamamoto, S., Moldrup, P., Kawamoto, K., & Komatsu, T. (2012). Organic matter fraction dependent model for predicting the gas diffusion coefficient in variably saturated soils. *Vadose Zone Journal*, 11. https://doi.org/10.2136/vzj2011.0065

Hamamoto, S., Ohko, Y., Ohtake, Y., Moldrup, P., & Nishimura, T. (2022). Water- and air-filled pore networks and transport parameters under drying and wetting processes. *Vadose Zone Journal*, 21, e20205. https://doi.org/10.1002/vzj2.20205

Haupenthal, A., Brax, M., Bentz, J., Jungkunst, H. F., Schützenmeister, K., & Kroener, E. (2021). Plants control soil gas exchanges possibly via mucilage. *Journal of Plant Nutrition and Soil Science*, 184(3), 320–328. https://doi.org/10.1002/jpln.202000496

Holz, M., Zarebanadkouki, M., Carminati, A., Hovind, J., Kaestner, A., & Spohn, M. (2019). Increased water retention in the rhizosphere allows for high phosphatase activity in drying soil. *Plant and Soil*, 443(1), 259–271. https://doi.org/10.1007/s11104-019-04234-3

Koestel, J., Larsbo, M., & Jarvis, N. (2020). Scale and REV analyses for porosity and pore connectivity measures in undisturbed soil. *Geoderma*, 366, 114206. https://doi.org/10.1016/j.geoderma.2020.114206

Kroener, E., Holz, M., Zarebanadkouki, M., Ahmed, M., & Carminati, A. (2018). Effects of mucilage on rhizosphere hydraulic functions depend on soil particle size. *Vadose Zone Journal*, 17(1), 170056. https://doi.org/10.2136/vzj2017.03.0056

Lazarovitch, N., Vanderborght, J., Jin, Y., & Van Genuchten, M. (2018). The root zone: Soil physics and beyond. *Vadose Zone Journal*, 17, 1–6. https://doi.org/10.2136/vzj2018.01.0002

Likos, W. J., Lu, N., & Godt, J. W. (2014). Hysteresis and uncertainty in soil water-retention curve parameters. *Journal of*

Geotechnical and Geoenvironmental Engineering, *140*(4), 04013050. https://doi.org/10.1061/(ASCE)GT.1943-5606.0001071

Liu, G., Li, B., Kelin, H., & van Genuchten, M. T. (2006). Simulating the gas diffusion coefficient in macropore network images: Influence of soil pore morphology. *Soil Science Society of America Journal*, *70*(4), 1252–1261.

Lucas, M., Vetterlein, D., Vogel, H.-J., & Schlüter, S. (2021). Revealing pore connectivity across scales and resolutions with X-ray CT. *European Journal of Soil Science*, *72*(2), 546–560. https://doi.org/10.1111/ejss.12961

Misiewicz, J., Głogowski, A., Lejcuś, K., & Marczak, D. (2020). The characteristics of swelling pressure for superabsorbent polymer and soil mixtures. *Materials*, *13*(22), 5071. https://doi.org/10.3390/ma13225071

Moldrup, P., Olesen, T., Gamst, J., Schjønning, P., Yamaguchi, T., & Rolston, D. E. (2000). Predicting the gas diffusion coefficient in repacked soil water-induced linear reduction model. *Soil Science Society of America Journal*, *64*(5), 1588–1594. https://doi.org/10.2136/sssaj2000.6451588x

Moradi, A. B., Carminati, A., Lamparter, A., Woche, S. K., Bachmann, J., Vetterlein, D., Vogel, H.-J., & Oswald, S. E. (2012). Is the rhizosphere temporarily water repellent? *Vadose Zone Journal*, *11*(3), vzj2011.0120. https://doi.org/10.2136/vzj2011.0120

Naveed, M., Ahmed, M. A., Benard, P., Brown, L. K., George, T. S., Bengough, A. G., Roose, T., Koebernick, N., & Hallett, P. D. (2019). Surface tension, rheology and hydrophobicity of rhizodeposits and seed mucilage influence soil water retention and hysteresis. *Plant and Soil*, *437*(1–2), 65–81. https://doi.org/10.1007/s11104-019-03939-9

Nazari, M. (2021). Plant mucilage components and their functions in the rhizosphere. *Rhizosphere*, *18*, 100344. https://doi.org/10.1016/j.rhisph.2021.100344

Renard, P., & Allard, D. (2013). Connectivity metrics for subsurface flow and transport. *Advances in Water Resources*, *51*, 168–196. https://doi.org/10.1016/j.advwatres.2011.12.001

Rivoal, J., & Hanson, A. D. (1994). Metabolic control of anaerobic glycolysis: Overexpression of lactate dehydrogenase in transgenic tomato roots supports the Davies-Roberts hypothesis and points to a critical role for lactate secretion. *Plant Physiology*, *106*(3), 1179–1185. https://doi.org/10.1104/pp.106.3.1179

Saha, A., Sekharan, S., & Manna, U. (2022). Hysteresis model for water retention characteristics of water-absorbing polymer-amended soils. *Journal of Geotechnical and Geoenviromental Engineering*, *148*, 04022008. https://doi.org/10.1061/(ASCE)GT.1943-5606.0002764

Thorbjørn, A., Moldrup, P., Blendstrup, H., Komatsu, T., & Rolston, D. E. (2008). A gas diffusivity model based on air-, solid-, and water-phase resistance in variably saturated soil. *Vadose Zone Journal*, *7*(4), 1276–1286. https://doi.org/10.2136/vzj2008.0023

Vogel, H. J. (1997). Morphological determination of pore connectivity as a function of pore size using serial sections. *European Journal of Soil Science*, *48*(3), 365–377. https://doi.org/10.1111/j.1365-2389.1997.tb00203.x

Vogel, H.-J. (2002). Topological characterization of porous media. In K. Mecke & D. Stoyan (Eds.), *Morphology of condensed matter* (Vol. 600, pp. 75–92). Springer. https://doi.org/10.1007/3-540-45782-8_3

Wen, T., Shao, L., & Guo, X. (2021). Effect of hysteresis on hydraulic properties of soils under multiple drying and wetting cycles. *European Journal of Environmental and Civil Engineering*, *25*(10), 1750–1762. https://doi.org/10.1080/19648189.2019.1600037

Wesseling, J., van Wijk, W. R., Fireman, M., van't Woudt, B. D., & Hagan, R. M. (1957). Land drainage in relation to soils and crops. In *Drainage of agricultural lands* (pp. 461–578). John Wiley & Sons, Ltd. https://doi.org/10.2134/agronmonogr7.c5

Wiegleb, G. (2016). *Physikalische Eigenschaften von Gasen*. Springer Vieweg.

Williams, K. A., Ruiz, S. A., Petroselli, C., Walker, N., McKay Fletcher, D. M., Pileio, G., & Roose, T. (2021). Physical characterisation of chia mucilage polymeric gel and its implications on rhizosphere science – Integrating imaging, MRI, and modelling to gain insights into plant and microbial amended soils. *Soil Biology and Biochemistry*, *162*, 108404.

Xu, X., Nieber, J. L., & Gupta, S. C. (1992). Compaction effect on the gas diffusion coefficient in soils. *Soil Science Society of America Journal*, *56*(6), 1743–1750. https://doi.org/10.2136/sssaj1992.03615995005600060014x

Zarebanadkouki, M., Fink, T., Benard, P., & Banfield, C. C. (2019). Mucilage facilitates nutrient diffusion in the drying rhizosphere. *Vadose Zone Journal*, *18*(1), 190021. https://doi.org/10.2136/vzj2019.02.0021

Zickenrott, I.-M., Woche, S. K., Bachmann, J., Ahmed, M. A., & Vetterlein, D. (2016). An efficient method for the collection of root mucilage from different plant species—A case study on the effect of mucilage on soil water repellency. *Journal of Plant Nutrition and Soil Science*, *179*(2), 294–302. https://doi.org/10.1002/jpln.201500511

SUPPORTING INFORMATION

Additional supporting information can be found online in the Supporting Information section at the end of this article.